Central European Geology, Vol. 57/4, 385–402 (2014)
DOI: 10.1556/CEuGeol.57.2014.4.4

Mineral chemistry of the ophiolitic peridotites and gabbros from the Serow area: Implications for tectonic setting and locating the Neotethys suture in NW Iran

Leyla Rezaii, Mohssen Moazzen*

Department of Earth Sciences, University of Tabriz, 51664, Tabriz, Iran

The Serow ophiolite in NW Iran, located at the Iran–Turkey border, is composed of mantle sequence peridotites, predominantly lherzolitic-harzburgite with subordinate amounts of lherzolite and dunite, and a crustal sequence made from gabbros, diabases, pillow lavas and deep marine carbonates and radiolarite sediments. The rocks appear as a tectonic mélange. This ophiolitic complex forms part of the ophiolites marking a branch of Neotethys oceanic crust in NW Iran. The chemistry of olivine, orthopyroxene and clinopyroxene in the lherzolitic-harzburgite and clinopyroxene in the gabbros suggests a supra-subduction setting for the ophiolite. The Serow ophiolite is similar to other ophiolites in NW Iran such as the Piranshahr, Naghadeh and Khoy and NE Turkey ophiolites in terms of the rock units, tectonic setting and age. The Serow ophiolite links the Iranian ophiolites from Baft in the SE through the South Azerbaijan suture to the Izmir–Ankara–Erzincan suture in the NW.

Key words: ophiolite, supra-subduction zone, lherzolitic-harzburgite, mineral chemistry, NW Iran

Introduction

The study of ophiolites as remnants of old oceanic crust fragments and plate margins is one of the interesting subjects in petrology, which together with plate tectonics helps in reconstructing geodynamic evolution. The eastern Mediterranean and Middle East contain numerous ophiolitic complexes within the Tethysides. Middle Jurassic

* Corresponding author: University of Tabriz, Tabriz, East Azerbaijan, Iran;
E-mail: moazzen@tabrizu.ac.ir
Received: May 4, 2014; accepted: November 4, 2014

ophiolites are exposed in Greece, East Turkey, Armenia and Iran. Remnants of the Paleotethys and Neotethys oceanic crust can be traced in three different zones in Iran.

The Alborz mountain range in North Iran is considered to be the Paleotethys suture (Zanchetta et al. 2009; Omrani et al. 2013), while ophiolitic exposures along the Zagros orogenic belt and those of Central Iran are related to the Neotethys closure (Stöcklin 1977). The main suture of the Neotethys closure is along the Zagros orogen in Iran, which extends to the northwest and is connected to the Ankara–Izmir–Erzincan and Bitlis Sutures (Fig. 1; Okay 1989; Okay and Tüysüz 1999; Göncüoglu et al. 2010; Moazzen et al. 2012). Ophiolites in NW Iran appear in the Khoy, Chaldoran, Serow, Salmas and Piranshahr areas. The Khoy ophiolites have been studied in greater detail (Hassanipak and Ghazi 2000; Azizi 2001; Azizi et al. 2002, 2006, 2011; Ghazi et al. 2003; Khalatbari-Jafari et al. 2003, 2004, 2005; Monsef et al. 2010). Two different scenarios can be considered for the Khoy ophiolites, based on these studies. In the first, they are considered to be a part of the Zagros-Bitlis Suture (Hassanipak and Ghazi 2000), also including the Troodos ophiolites in Cyprus, the Barebassite ophiolites in Syria, Kizil Dag and Cilo, the Hatay ophiolites in Turkey and the Neyriz and Kermanshah ophiolites in Iran. In the second scenario, proposed by Kananian et al. (2001), the Khoy ophiolites are considered as the continuation of Inner Iran ophiolites such as the Nain, Shahrbabk, Sabzevar and Band-e-Zeyarat ophiolites, also known as the Kahnuj ophiolites, which are considered to be the result of the closure of a Neotethys seaway in the Mesozoic between the Sanandaj-Sirjan metamorphic belt and the Central Iran Block. Studies by Khalatbari-Jafari et al. (2003) indicate two

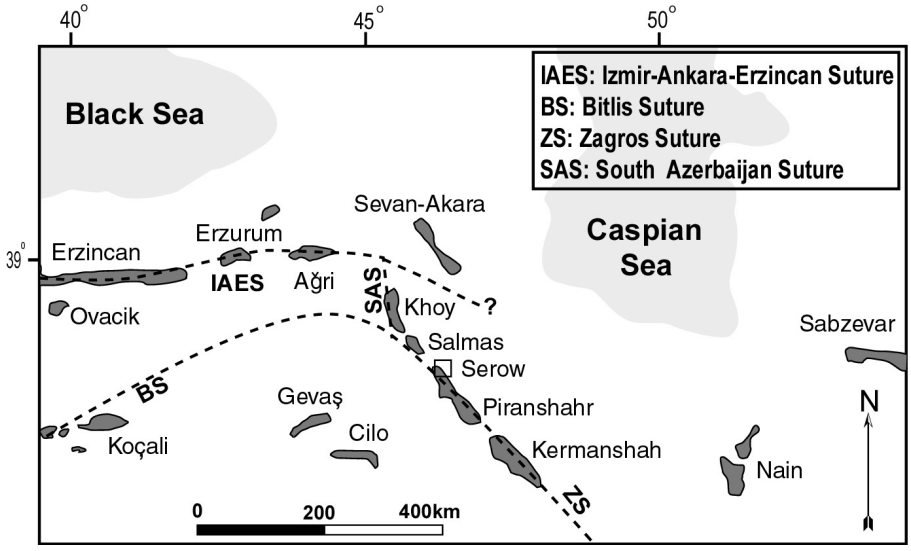

Fig. 1
The main Neo-Tethyan sutures in NE Turkey and NW Iran (from Topuz et al. 2013a). The study area is shown by a rectangle

different ophiolitic complexes in the Khoy area: one is the metamorphosed ophiolitic complex of Lower to Middle Jurassic age and the other is the non-metamorphosed ophiolitic complex of Upper Cretaceous age. Monsef et al. (2010) reported a supra-subduction setting for the metamorphosed ophiolitic complex. Also, Alchalan (2011) considers that the non-metamorphosed ophiolitic complex was formed in a supra-subduction zone, based on the mineral chemistry of peridotites. Toward the west the Refahiye (Topuz et al. 2013a, b) and Eldivan (Çelik et al. 2011, 2013) ophiolites in Turkey are supra-subduction types.

The ophiolites from the Serow area are of great importance in the reconstruction of the geodynamic evolution of the Tethysides in NW Iran and adjacent areas. There are no published data on the petrology and tectonic setting of this ophiolitic complex. We have studied the mineral chemistry of peridotites from the mantle sequence and gabbros from the crustal sequence of the Serow ophiolite in order to reveal its geodynamic and tectonic evolution. The results will be used to work out the possibility of connecting the NW Iran ophiolites to those in eastern Turkey along the Izmir–Ankara–Erzincan Suture. This will help locate the Neotethys suture more precisely in NW Iran.

Geologic background and petrography

The rock units in the Serow area can be grouped into two main categories. The first group includes non-ophiolitic rocks and the second group comprises an ophiolitic complex. Non-ophiolitic rocks are pre-Upper Cambrian polymetamorphic and mylonitized marbles, gneisses and skarns (Fig. 2) and post-Upper Cambrian leucogranites, alkaligranites, dolomites and limestones. The ophiolitic complex is the main Mesozoic (Cretaceous) unit in the area. Tertiary rocks include coarse-grained conglomerates, Paleocene to Early Eocene sandstones and limestones and Neogene conglomerates.

The Mesozoic ophiolitic complex appears as a tectonic ophiolite mélange made of partially serpentinized peridotites, pillow lavas, radiolarite and pelagic limestones, Upper Cretaceous *globotruncana*-bearing limestones, and finely laminated alterations of limestone, shale, and sandstone of Cretaceous age. Partially serpentinized peridotites are one of the main rock types of the ophiolitic mélange, which cover vast areas (Fig. 3). Based on the mineralogy and texture due to serpentinization, they are predominantly lherzolitic-harzburgites with subordinate amounts of lherzolites and dunites. Gabbros appear as blocks within a serpentine matrix in the ophiolitic mélange. The peridotites are composed of olivine, orthopyroxene, clinopyroxene and opaque minerals (Cr-spinel) as primary mantle phases. Orthopyroxene and olivine are the main mineral phases, while clinopyroxene appears as a subordinate phase. Mesh texture is developed due to serpentinization of olivine (Fig. 4a, b) and bastite is developed after pyroxene. Orthopyroxene exsolution in clinopyroxene can be seen in the samples as lamellae (Fig. 4c). Clinopyroxene appears as relatively larger crystals in some samples (Fig. 4d). Under the microscope, the gabbros consist of high modal percentage of plagioclase (50–60 modal%) and pyroxene (30–35 modal%). The studied gabbro

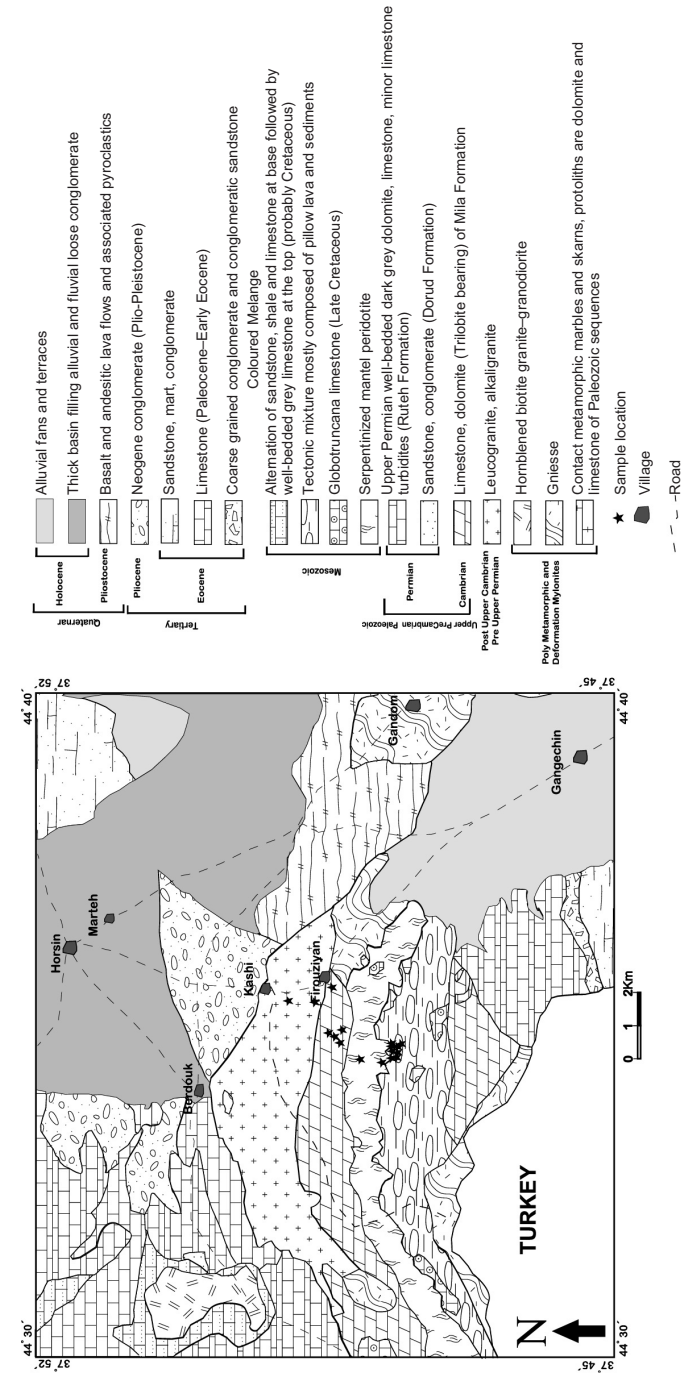

Fig. 2
Geologic map of the Serow area adopted from the 1:100,000 Gengchin map (Geological Survey of Iran)

Fig. 3
Outcrop of serpentinized peridotites and pelagic limestone in the Serow area

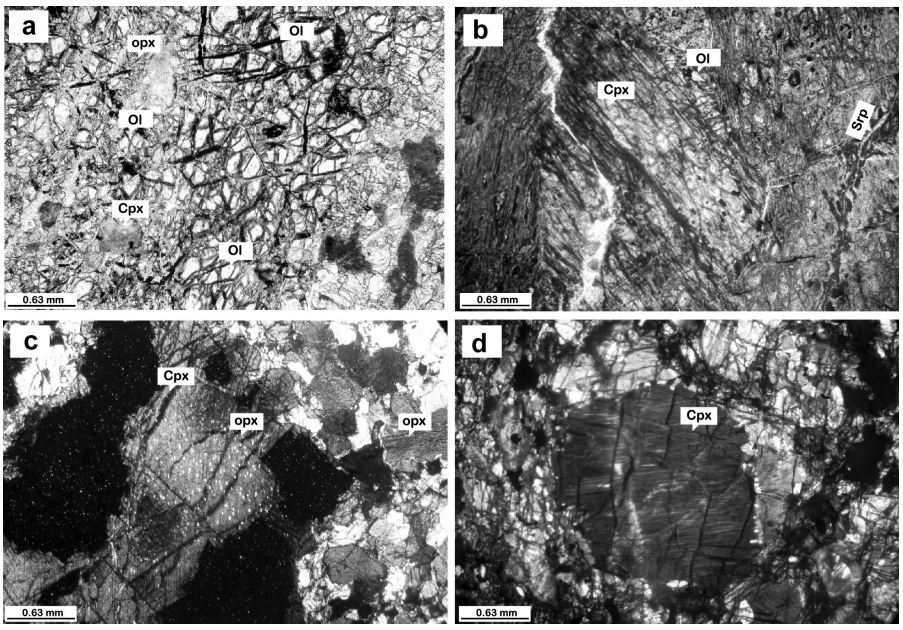

Fig. 4
Mineral composition and textural relations in the Serow area ultramafic rocks. a: Olivine, clinopyroxene and orthopyroxene in peridotites; b: mesh texture in olivine developed by serpentinization; c: orthopyroxene exclusion lamellae in clinopyroxene; d: bastite texture after clinopyroxene. All photos in XPL. Abbreviations for the mineral names are from Whitney and Evans (2010)

samples lack olivine. Some plagioclase crystals are partially altered to sericite and/or clay minerals (Fig. 5a). Pyroxenes are converted to tremolite-actinolite from the rims and at fractures due to late hydration. Chlorite is also a product of late alteration in these rocks (Fig. 5b).

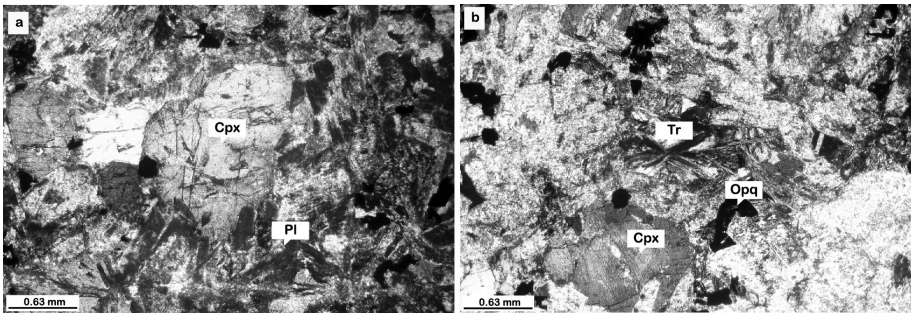

Fig. 5
a: Clinopyroxene and plagioclase in the gabbroic samples; b: Alternation of clinopyroxene to tremolite in gabbroic samples. Plagioclase is slightly altered to sericite. Abbreviations for the mineral names are from Whitney and Evans (2010)

Applied methods

In order to work out the mineralogical features and to determine the tectonic setting of the studied rocks, pyroxene and olivine were analyzed in ultramafic and mafic samples. Olivine and clinopyroxene are analyzed in lherzolitic-harzburgite, and clinopyroxene in gabbro samples. Representative, optically well-studied samples of peridotite and gabbro were analyzed with a JEOL JXA-8800 microprobe at Potsdam University. An accelerating voltage of 15 KV, a specimen current of 20 nA and current diameter of 1–3 μm were used. In order to obtain representative analysis of clinopyroxene with orthopyroxene lamellae, a relatively broader beam was applied to cover both host mineral and the lamellae. Counting time was 30 seconds on peaks and half-peak on background. Natural and synthetic standards (Fe_2O_3 [Fe], rhodonite [Mn], rutile [Ti], MgO [Mg], wollastonite [Si, Ca], fluorite [F], orthoclase [Al, K] and albite [Na]) were used for calibration. The Fe^{2+}/Fe^{3+} ratio is calculated based on stoichiometry (Droop 1987).

Mineral chemistry

Representative mineral chemical data are presented in Tables 1 to 3. The composition of olivine in partially serpentinized lherzolitic-harzburgite is $Fo_{85.6–86.7}$. The average of Mg# (Mg/(Mg + Fe^{2+}) is 0.86; according to the Fo-Fa diagram of Deer et al. (1992) the analyzed olivines are chrysolite. The orthopyroxene average composition in the lherzolitic-harzburgite samples is $Wo_{0.2}Fs_{0.1}En_{0.7}$ and the Mg# is 0.87–0.90.

Plotting these compositions on the En-Fs-Wo triangular diagram of Morimoto et al. (1988) shows that the orthopyroxenes are enstatite (Fig. 6).

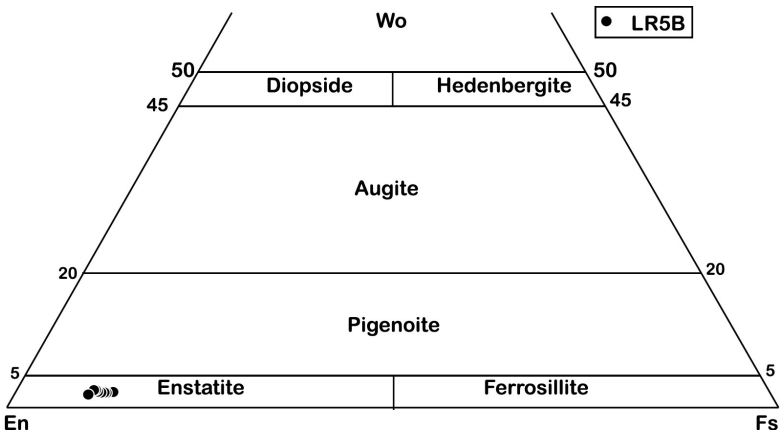

Fig. 6
Composition of the analyzed orthopyroxenes in the lherzolites on En-Fs-Wo diagram (Morimoto et al. 1988). All samples plot in the enstatite field

The average composition of clinopyroxene in the mafic (gabbro) samples is $Wo_{0.38–0.46}Fs_{0.05–0.15}En_{0.44–0.51.}$ The end-member composition of the studied clinopyroxene in the lherzolitic-harzburgite samples is $Wo_{0.46–0.49}Fs_{0.02–0.04}En_{0.48–0.50.}$ Mg# calculated for clinopyroxene in gabbro samples is 0.74–0.92 and Mg#; for clinopyroxene in lherzolitic-harzburgite samples it is 0.92–0.96. According to the classification diagram of Morimoto et al. (1988) clinopyroxene of the gabbro samples are augites and those in the lherzolitic-harzburgite are diopsides (Fig. 7a). Classification

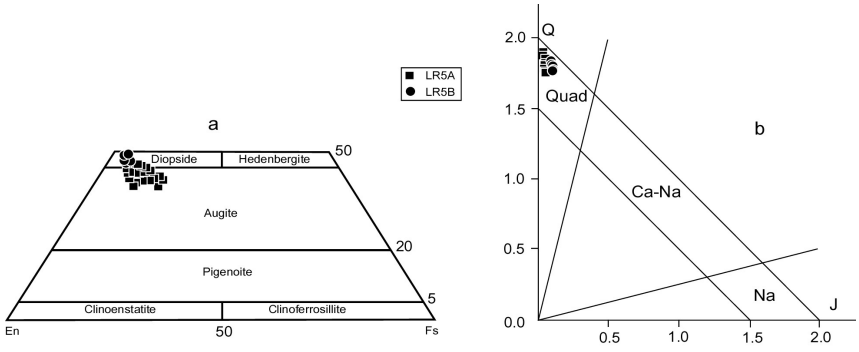

Fig. 7
a. Composition of analyzed clinopyroxenes in the mafic and umtramafic samples of the Serow ophiolites on the En-Fs-Wo diagram of Morimoto et al. (1988). Clinopyroxenes in the mafic sample (gabbro) are augite, and diopside in the lherzolite; b. Classification of clinopyroxenes based on Q and J parameters (Morimoto et al. 1988). All samples are of Quad type

of clinopyroxenes based on Q = Mg + Ca + Fe^{+2} and J = 2Na factors (Morimoto et al. 1988) show that all clinopyroxenes in both lherzolitic-harzburgite and gabbro samples plot in the Quad field, indicating that the studied clinopyroxenes are poor in Na end-members (Fig. 7b).

Table 1
Representative mineral chemistry and formula unit for analyzed olivine crystals in the lherzolitic-harzburgite. Major oxides in wt%

Sample	1	2	3	4	5	6	7	8	9	10	11
SiO_2	40.04	39.72	39.83	39.68	39.74	39.49	39.97	39.66	39.81	39.86	39.60
TiO_2	0.01	0.02	BD	0.01	0.03	0.03	0.02	BD	0.02	BD	0.02
Al_2O_3	BD	0.01	BD	0.01	BD	BD	BD	BD	0.01	BD	BD
Cr_2O_3	0.02	BD	BD	0.03	0.03	BD	0.02	0.01	0.01	0.03	0.02
FeO	14.00	13.88	14.08	13.88	13.48	13.95	13.90	14.02	13.91	14.10	13.92
MnO	0.18	0.19	0.16	0.18	0.17	0.19	0.19	0.19	0.15	0.14	0.19
MgO	47.16	46.84	47.30	47.59	47.26	46.86	47.79	46.87	47.63	47.76	47.12
CaO	0.02	0.02	0.01	0.02	0.02	0.02	0.03	0.02	0.02	0.03	0.02
Na_2O	BD	BD	BD	BD	BD	0.01	BD	BD	BD	BD	BD
NiO	0.01	0.01	0.01	BD	BD	0.01	0.01	0.01	0.01	0.01	0.01
Total	101.44	100.70	101.40	101.38	100.75	100.57	101.91	100.79	101.57	101.92	100.89
Si	0.99	0.98	0.98	0.98	0.98	0.98	0.98	0.98	0.98	0.98	0.98
Ti	0.00	0.00	0.00	0.00	0.00	0.00	0.00	0.00	0.00	0.00	0.00
Al	0.00	0.00	0.00	0.00	0.00	0.00	0.00	0.00	0.00	0.00	0.00
Cr	0.00	0.00	0.00	0.00	0.00	0.00	0.00	0.00	0.00	0.00	0.00
Fe^{++}	0.29	0.29	0.29	0.29	0.28	0.29	0.28	0.29	0.29	0.29	0.29
Mn	0.00	0.00	0.00	0.00	0.00	0.00	0.00	0.00	0.00	0.00	0.00
Mg	1.73	1.73	1.74	1.75	1.74	1.74	1.74	1.73	1.74	1.74	1.74
Ca	0.00	0.00	0.00	0.00	0.00	0.00	0.00	0.00	0.00	0.00	0.00
Na	0.00	0.00	0.00	0.00	0.00	0.00	0.00	0.00	0.00	0.00	0.00
K	0.00	0.00	0.00	0.00	0.00	0.00	0.00	0.00	0.00	0.00	0.00
Ni	0.01	0.01	0.01	0.00	0.01	0.01	0.01	0.01	0.01	0.01	0.01
Total	3.01	3.02	3.02	3.02	3.02	3.02	3.02	3.02	3.02	3.02	3.02
Mg#	0.86	0.86	0.86	0.86	0.86	0.86	0.86	0.86	0.86	0.86	0.86
Fo	85.72	85.74	85.69	85.94	86.21	85.69	85.97	85.63	85.92	85.79	85.79
Fa	14.28	14.26	14.31	14.06	13.79	14.31	14.03	14.37	14.08	14.21	14.21

BD = Below Detection Limit

Discussion

Clinopyroxene is a useful mineral in determining the tectonic setting (Leterrier et al. 1982), magmatic series and tectonomagmatic features (Beccaluva et al. 1989), as well as the pressure and temperature condition of crystallization of the rocks containing this mineral (Soesoo 1997). Application of Al^{VI} vs. Al^{IV} for clinopyroxenes (Aoki and Shiba 1973) in gabbroic samples show low to moderate pressure for formation of the gabbros (Fig. 8a). Helz (1973) showed that Al distribution in tetrahedral and octahedral sites of clinopyroxene is indicative in terms of water content of the parental

Table 2
Representative mineral chemistry (wt%) and unit formula of orthopyroxene in the ultramafic rocks

Sample	1	2	3	4	5	6	7	8	9	10	11
SiO_2	54.59	53.93	54.85	54.74	54.81	55.24	55.09	54.56	55.34	55.26	54.66
TiO_2	0.30	0.28	0.32	0.30	0.32	0.29	0.30	0.33	0.29	0.33	0.27
Al_2O_3	2.28	2.23	2.21	2.32	2.25	1.92	1.94	2.28	1.84	2.40	1.84
Cr_2O_3	0.45	0.43	0.39	0.41	0.46	0.30	0.32	0.44	0.31	0.42	0.34
FeO	9.17	9.30	9.17	9.01	9.41	9.22	9.29	9.35	9.12	9.29	9.20
MnO	0.17	0.20	0.19	0.18	0.15	0.15	0.18	0.21	0.21	0.18	0.17
MgO	32.17	31.38	32.49	32.12	32.26	32.40	31.86	31.96	32.46	31.60	31.72
CaO	1.00	1.16	0.95	1.18	1.22	0.94	0.91	0.96	0.81	1.09	0.93
Na_2O	0.01	0.04	0.01	0.02	0.03	0.03	0.01	0.01	BD	0.02	0.01
Total	100.14	98.94	100.59	100.28	100.91	100.50	99.91	100.10	100.38	100.59	99.13
Si	1.90	1.91	1.90	1.91	1.90	1.92	1.93	1.91	1.92	1.92	1.93
Ti	0.01	0.01	0.01	0.01	0.01	0.01	0.01	0.01	0.01	0.01	0.01
Al	0.09	0.09	0.09	0.10	0.09	0.08	0.08	0.09	0.08	0.10	0.08
Cr	0.01	0.01	0.01	0.01	0.01	0.01	0.01	0.01	0.01	0.01	0.01
Fe^{3+}	0.07	0.07	0.08	0.07	0.09	0.06	0.04	0.07	0.05	0.03	0.04
Fe^{2+}	0.20	0.20	0.19	0.19	0.19	0.20	0.23	0.21	0.21	0.24	0.23
Mn	0.00	0.01	0.01	0.01	0.00	0.00	0.01	0.01	0.01	0.01	0.00
Mg	1.67	1.65	1.68	1.67	1.67	1.68	1.66	1.66	1.68	1.64	1.67
Ca	0.04	0.04	0.04	0.04	0.05	0.03	0.03	0.04	0.03	0.04	0.04
Na	0.00	0.00	0.00	0.00	0.00	0.00	0.00	0.00	0.00	0.00	0.00
K	0.00	0.00	0.00	0.00	0.00	0.00	0.00	0.00	0.00	0.00	0.00
Total	4.00	4.00	4.00	4.00	4.00	4.00	4.00	4.00	4.00	4.00	4.00
+Mg/ (Mg+Fe^2)	0.90	0.89	0.90	0.90	0.90	0.89	0.88	0.89	0.89	0.87	0.88
Fe^{2+}/ (Fe^{tot})	0.73	0.74	0.71	0.74	0.69	0.76	0.86	0.76	0.80	0.90	0.83
Al/(Al+ Fe^{3+}+Cr)	0.53	0.53	0.51	0.54	0.48	0.53	0.63	0.54	0.55	0.72	0.58
En	0.88	0.87	0.88	0.88	0.88	0.87	0.86	0.87	0.87	0.85	0.86
Fs	0.10	0.11	0.10	0.10	0.10	0.11	0.12	0.11	0.11	0.13	0.12
Wo	0.02	0.02	0.02	0.02	0.02	0.02	0.02	0.02	0.02	0.02	0.02
Jd	0.00	0.00	0.00	0.00	0.00	0.00	0.00	0.00	0.00	0.00	0.00
Ac	0.00	0.00	0.00	0.00	0.00	0.00	0.00	0.00	0.00	0.00	0.00
Aug	1.00	1.00	1.00	1.00	1.00	1.00	1.00	1.00	1.00	1.00	1.00

BD = Below Detection Limit

magma. Al^{IV} vs. Al^{VI} for clinopyroxenes in the gabbros from the Serow area (Fig. 8b) reveals that the rocks crystallized from a magma containing ~10 wt% water. Clinopyroxenes in the gabbros plot adjacent to the $Fe^{3+} = 0$ line on the $Na+Al^{IV}$ vs. $Al^{IV} + 2Ti + Cr$ diagram (Schweitzer et al. 1974), indicating moderate oxygen fugacity during pyroxene crystallization (Fig. 9).

The SiO_2 versus Al_2O_3 diagram (Le Bas 1962) for clinopyroxenes in the mafic rocks (gabbros) from the Serow ophiolites indicates that the original magma was alkaline/sub-alkaline in nature (Fig. 10a). On the F1 versus F2 parameters (Nisbet and

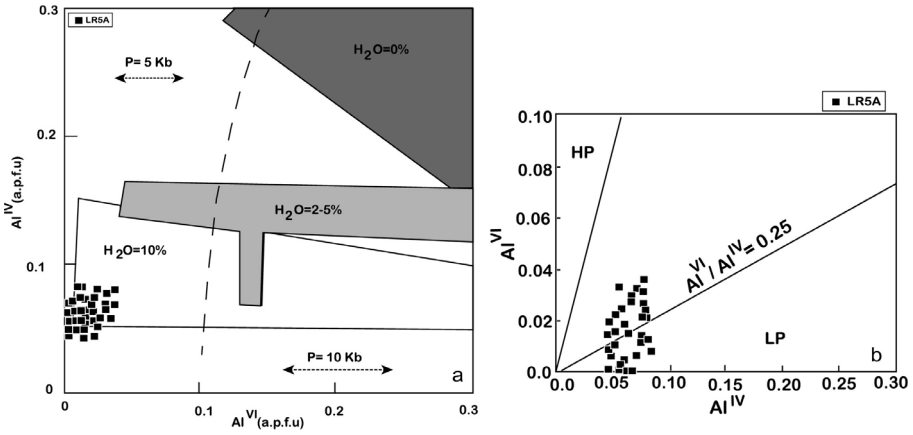

Fig. 8
a. Al^{IV} versus Al^{VI} diagram (Aoki and Shiba 1973) for clinopyroxenes in the Serow gabbros, which indicates low to medium pressure for crystallization; b. Al^{IV} versus Al^{VI} diagram of Helz (1973) shows that the gabbros were crystallized from a magma in equilibration with ~10 wt% H_2O

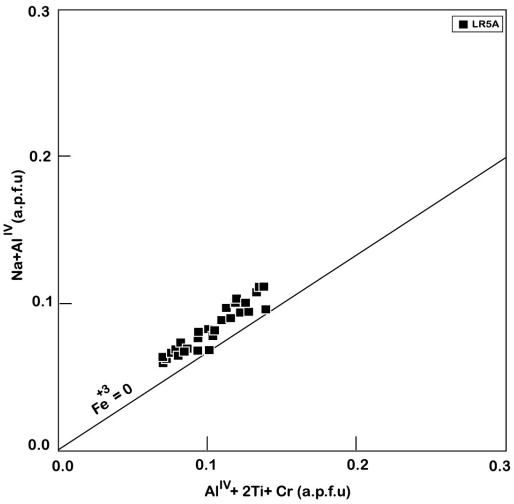

Fig. 9
$Na + Al^{IV}$ against $Al^{IV}+ 2Ti + Cr$ diagram (Schweitzer et al. 1974) for the clinopyroxenes in the Serow gabbros indicating slightly oxidized condition for the rock crystallization

Pearce 1977), the gabbros show ophiolitic basalt and intra-plate tholeiite characteristics (Fig. 10b). The composition of the clinopyroxene in the peridotites defines an oceanic environment, i.e. they represent peridotites located beneath the oceanic lithosphere (Fig. 11). Mg# versus Cr_2O_3 wt% in clinopyroxene (Johnson et al. 1990; Ishii et al. 1992) shows that the peridotites have fore-arc affinities (Fig. 12a). Also, in the Al^{IV} versus Ti diagram of Beccaluva et al. (1989) for the clinopyroxenes, an island arc setting can be deduced for the peridotites and the ophiolitic complex. It is obvious from this diagram that the samples plot very close to the boninite field (Fig. 12b).

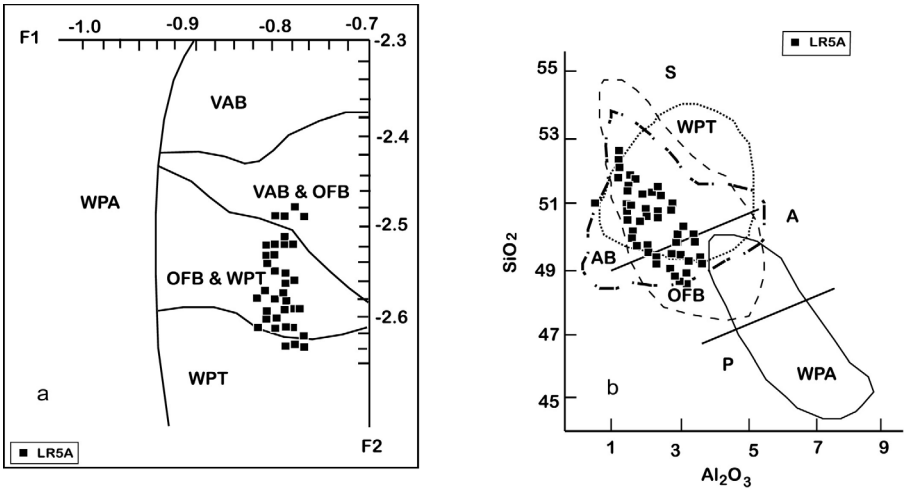

Fig. 10
a. Discrimination of the magmatic series using clinopyroxene chemistry (Le Bas 1962). The analyzed data plot in the alkaline and sub-alkaline fields and on the joint field of intra-plate tholeiites, arc basalt and ophiolite basalt; b. F1 versus F2 diagram (Nisbet and Pearce 1977) indicates that mafic rocks from the Serow ophiolite plot mainly in the ophiolite basalt and within plate tholeiite fields

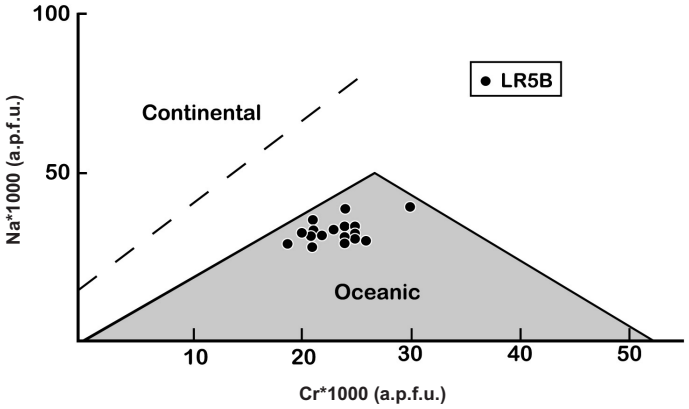

Fig. 11
Na versus Cr diagram for clinopyroxene (Kornprobst et al. 1981) showing an oceanic environment for the Serow peridotites

Regarding the mineral chemistry of olivine and pyroxene in the mafic and ultramafic rocks from the Serow ophiolites, it can be concluded that the rocks were formed at a supra-subduction zone setting in the fore-arc environment. Abyssal and supra-subduction zone peridotites are characterized by distinct mineralogical and geochemical features. Abyssal peridotites are generally made from lherzolites and clino-

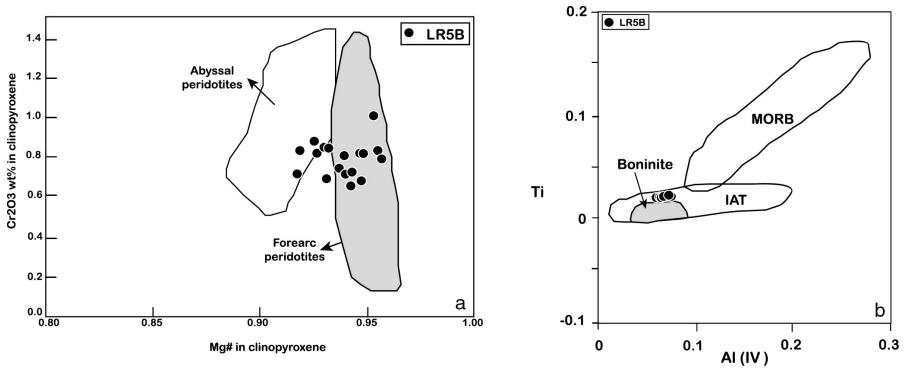

Fig. 12
a. Mg# against Cr_2O_3 for peridotites indicating the abyssal peridotites field (Johnson et al. 1990) and fore arc setting (Ishii et al. 1992). Data from the studied samples plot mainly in the forearc peridotites field; b. Al^{IV} versus Ti diagram for clinopyroxenes (Beccaluva et al. 1989), which indicates that the Serow peridotites were from an island arc setting and of boninitic nature

pyroxene-rich harzburgites, formed by MORB-type melt extraction as a result of partial melting of fertile mantle under dry conditions (e.g. Dick and Bullen 1984; Johnson and Dick 1992). Supra-subduction zone peridotites are mainly depleted harzburgite or lherzolitic-harzburgite. They are the remnants of much higher degrees of partial melting of the upper mantle above a subducting slab (e.g. Aldanmaz et al. 2009). Olivine in these harzburgites is characterized by higher forsterite content. The forsterite content of the Serow olivines is more than 85 mol %. Pyroxenes in supra-subduction zone-type peridotites are also expected to be depleted in elements such as Al, Cr and Na due to the higher degrees of partial melting. Cr_2O_3 content in the studied orthopyroxene ranges from 0.30 to 0.46 wt%, which is low. Cr_2O_3 content of the clinopyroxenes is 0.73 to 1.02 wt%. Na_2O content of the orthopyroxene and clinopyroxene is 0.01 to 0.04 and 0.46 to 0.60 wt%, respectively. The Al_2O_3 content is relatively high in comparison with Al_2O_3 content in pyroxenes from the highly depleted supra-subduction zone harzburgites. Al_2O_3 content is 1.84 to 2.32 wt% in the analyzed orthopyroxene and 3.37 to 4.07 in the studied clinopyroxenes (Table 3). These chemical features show that the Serow peridotites are not highly depleted. This is in accordance with the petrography (presence of clinopyroxene in the samples). Considering a supra-subduction zone setting for the Serow peridotites, they are expected to be depleted ones, while the studied peridotites are only moderately depleted.

Studies on supra-subduction zone ophiolites have shown that the mafic and ultramafic rocks in this tectonic setting are heterogeneous in composition. This indicates a complex melt extraction, leaving peridotites with different degrees of depletion behind. These supra-subduction zone ophiolites likely are formed in initial stages of subduction (Beccaluva et al. 1994; Bédard et al. 1998; Godard et al. 2003; Encarnacion 2004; Dilek and Thy 2009). Different studies show progressive changes of ophiolitic magmas from MORB to island arc tholeiites and boninites, from the arc

Table 3
Representative mineral chemistry (wt%) of clinopyroxene in the mafic and ultramafic samples

Sample	Lherzolite						Gabbro					
SiO_2	51.29	51.50	51.02	50.72	50.62	51.03	52.65	50.09	52.21	51.94	49.78	51.34
TiO_2	0.88	0.74	0.86	0.77	0.92	0.86	0.36	0.45	0.39	0.57	0.91	0.40
Al_2O_3	3.54	3.37	3.51	3.85	4.07	3.68	2.33	3.05	2.36	2.30	3.26	2.97
Cr_2O_3	0.83	0.73	0.84	0.86	1.02	0.84	0.34	0.04	0.30	0.04	BD	0.64
FeO	4.50	4.15	3.92	4.37	4.09	4.37	5.90	7.83	5.74	9.35	12.21	5.16
MnO	0.11	0.10	0.12	0.13	0.12	0.12	0.16	0.18	0.15	0.25	0.36	0.16
MgO	16.90	16.29	16.32	15.82	16.05	16.30	17.71	15.67	17.41	17.23	14.31	17.02
CaO	21.32	22.54	22.55	22.36	22.18	21.55	20.70	21.33	21.22	18.30	18.77	21.36
Na_2O	0.46	0.53	0.50	0.49	0.60	0.52	0.24	0.21	0.22	0.27	0.35	0.24
Total	99.83	99.94	99.64	99.37	99.66	99.27	100.38	98.86	100.01	100.26	99.95	99.30
Si	1.87	1.88	1.87	1.86	1.85	1.88	1.91	1.87	1.91	1.91	1.86	1.89
Ti	0.02	0.02	0.02	0.02	0.03	0.02	0.01	0.01	0.01	0.02	0.03	0.01
Al	0.15	0.14	0.15	0.17	0.18	0.16	0.10	0.13	0.10	0.10	0.14	0.13
Cr	0.02	0.02	0.02	0.03	0.03	0.02	0.01	0.00	0.01	0.00	0.00	0.02
Fe^{3+}	0.06	0.07	0.08	0.07	0.08	0.05	0.06	0.12	0.07	0.07	0.11	0.07
Fe^{2+}	0.07	0.05	0.04	0.06	0.04	0.08	0.12	0.12	0.10	0.21	0.28	0.08
Mn	0.00	0.00	0.00	0.00	0.00	0.00	0.00	0.01	0.00	0.01	0.01	0.00
Mg	0.92	0.89	0.89	0.87	0.88	0.89	0.96	0.87	0.95	0.94	0.80	0.93
Ca	0.83	0.88	0.88	0.88	0.87	0.85	0.81	0.85	0.83	0.72	0.75	0.84
Na	0.03	0.04	0.04	0.04	0.04	0.04	0.02	0.02	0.02	0.02	0.03	0.02
K	0.00	0.00	0.00	0.00	0.00	0.00	0.00	0.00	0.00	0.00	0.00	0.00
Total	4.00	4.00	4.00	4.00	4.00	4.00	4.00	4.00	4.00	4.00	4.00	4.00
Mg/ (Mg+Fe^{2+})	0.93	0.94	0.96	0.93	0.95	0.92	0.89	0.88	0.90	0.82	0.74	0.92
Fe^{2+}/ (Fe^{tot})	0.53	0.43	0.35	0.47	0.35	0.60	0.67	0.49	0.59	0.74	0.72	0.53
Al/(Al+ Fe^{3+}+Cr)	0.63	0.61	0.60	0.63	0.61	0.67	0.59	0.52	0.56	0.57	0.57	0.58
En	0.50	0.49	0.49	0.48	0.49	0.49	0.51	0.47	0.50	0.50	0.44	0.50
Fs	0.04	0.03	0.02	0.03	0.02	0.04	0.06	0.07	0.05	0.11	0.15	0.05
Wo	0.46	0.48	0.49	0.49	0.49	0.47	0.43	0.46	0.44	0.38	0.41	0.45
Jd	0.02	0.02	0.02	0.02	0.03	0.02	0.01	0.01	0.01	0.01	0.01	0.01
Ac	0.01	0.01	0.01	0.01	0.02	0.01	0.01	0.01	0.01	0.01	0.01	0.01
Aug	0.97	0.96	0.96	0.96	0.96	0.96	0.98	0.98	0.98	0.98	0.97	0.98

BD = Below Detection Limit

toward the trench (e.g. Dilek et al. 2008; Dilek and Thy 2009). These changes are a result of various degrees of melting of a highly heterogeneous and repeatedly depleted mantle source. This source is usually modified by slab-derived fluids (Dilek and Thy 2009). The relatively high H_2O content for the melt crystallizing the Serow ophiolitic gabbros (~10 wt%) determined above can show that the magma was formed in a supra-subduction setting and became enriched in fluids exerting from descending-slab dehydration. These observations are similar to the evolution of the Izu–Bonin–

Mariana forearc (Pearce et al. 1992; Van der Lann et al. 1992; Bloomer et al. 1995; Cosca et al. 1998).

The moderately depleted peridotites from the Serow area can be considered as samples representing heterogeneous mantle sources in a supra-subduction setting. They could also have formed by re-fertilization processes acting on earlier depleted harzburgite. There is no textural evidence for re-fertilization in the studied samples. Therefore they are more likely part of a heterogeneous mantle assemblage as shown by Dilek and Thy (2009).

Supra-subduction zone ophiolites are far better represented and preserved than MORB ophiolites in the orogenic belts. There are two main ophiolitic belts along the Zagros orogen in Iran. These are the "outer" ophiolitic belt including the Kermanshah, Neyriz and Esfandagheh ophiolites, cropping out to the south of the Main Zagros Thrust, and the "inner" ophiolitic belt including the Baft, Dehshir, Shahr Babak and Nian ophiolites (Fig. 13). The "inner" ophiolite belt lies along the southwest margin of the Central Iranian Block. All rock units of the crustal and the mantle sequences of the "inner" and "outer" Zagros ophiolitic belts are characterized by strong supra-subduction zone compositional features (Shafaii Moghadam and Stern 2011).

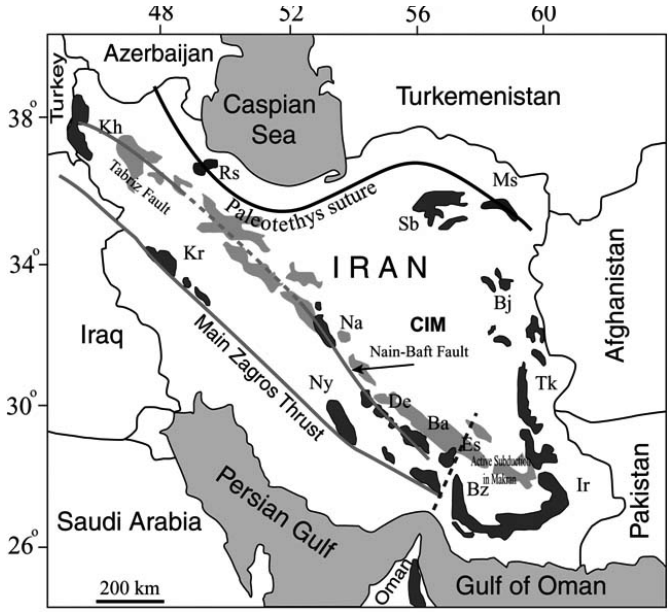

Fig. 13
Distribution of ophiolites in Iran and possible connection of SE Zagros ophiolites in the Baft area to those along the NW trend to the Khoy ophiolites. Abbreviations show ophiolites in these areas. Ir: Iranshahr, Bz: Bazman, Tk: Tchehel-Kureh, Bj: Birjand, Ms: Mashad, Sb: Sabzevar, Rs: Rasht, Es: Esfandagheh, Bs: Baft, De: Dehshir, Na: Nain, Kh: Khoy, Kr: Kermanshah and Ny: Neyriz

Regarding the studies of the peridotites and the crustal sequence of the ophiolites in Baft (Arvin and Robinson 1994), Dehshir (Shafaii Moghadam et al. 2010), Shahr Babak (Ghazi and Hassanipak 2000) and Nain (Mehdipour Ghazi et al. 2010) areas (Fig. 13), it is demonstrated that these ophiolites were formed in an arc setting (supra-subduction zone). Ophiolites from the west of Khoy (Alchalan 2011), Naghadeh (Ilkhani 2013) and Piranshahr (Hajialioghli and Moazzen 2014) in NW Iran were formed in a supra-subduction zone as well. Therefore it is reasonable to consider all these ophiolites, which are similar in terms of petrography, geochemistry, age and tectonic setting, as representing a single suture. If this is the case, the Neotethys suture zone with a supra-subduction feature is running from Baft in the SE of Iran to the Khoy area in the NW. Probably most of this suture is covered by products of young volcanic activities toward the NW. This branch of the Neotethys was called the Baft-Khoy seaway by Moazzen et al. (2012) (Fig. 13). Ophiolites along the Izmir–Ankara–Erzincan suture are mainly supra-subduction ones (e.g. Okay and Tüysüz 1999; Göncüoglu et al. 2010) and share very similar features with the Baft-Khoy ophiolites of Iran. The Serow ophiolites link these two together. It can be postulated that the Baft-Khoy suture is connected to the Izmir–Ankara–Erzincan suture by the Serow ophiolites through the South Azerbaijan Suture (cf. Fig. 1).

Acknowledgements

This contribution is a part of the M.Sc. thesis of the primary author. Field work was supported by the University of Tabriz. We thank Dr. Roland Oberhänsli and Dr. Uwe Altenberger for their help and encouragement. Dr. Attila Demény and Dr. Tivadar M. Tóth are acknowledged for their guidance and editorial help. Constructive comments by two anonymous reviewers improved the manuscript.

References

Alchalan, S. 2011: Investigations on metabasic and ultrabasic rocks from west Khoy-NW Iran. – M.Sc. Thesis, University of Tabriz, Iran, 114 pp.

Aldanmaz, E., M.W. Schmidt, A. Gourgaud, T. Meisel 2009: Mid-ocean ridge and supra-subduction geochemical signatures in spinel-peridotites from the Neotethyan ophiolites in SW Turkey: Implications for upper mantle melting processes. – Lithos, 113, pp. 691–708.

Aoki, K., I. Shiba 1973: Pargasites in lherzolite and websterite inclusions from Itinome-gata, Japan. – Journal of Japan Association of Mineralogy, Petrology, Economic Geology, 68, pp. 303–310.

Arvin, M., P.T. Robinson 1994: The petrogenesis and tectonic setting of lavas from the Baft Ophiolitic Melange, southwest of Kerman, Iran. – Canadian Journal of Earth Sciences, 31, pp. 824–834.

Azizi, H. 2001: Petrography, Petrology and Geochemistry of the Khoy Metamorphic Rocks. PhD Thesis (in Farsi). – University of Tarbiat Moalem, Tehran, Iran, 255 pp.

Azizi, H., H. Moinevaziri, M. Noghreayan 2002: Geochemistry of metabasites in the north of Khoy. – Journal of Sciences (in Farsi), University of Isfahan, Iran, 15, pp. 1–20.

Azizi, H., H. Moinevaziri, M. Mohajjel, A. Yagobpoor 2006: PTt path in metamorphic rocks of the Khoy region (northwest Iran) and their tectonic significance for Cretaceous–Tertiary continental collision. – Journal of Asian Earth Sciences, 27, pp. 1–9.

Azizi, H., S. Chung, T. Tanaka, Y. Asahara 2011: Isotopic dating of the Khoy metamorphic complex (KMC), northwestern Iran: A significant revision of the formation age and magma source. – Precambrian Research, 185, pp. 87–94.

Beccaluva, L., M. Coltorti, I. Premti, E. Saccani, F. Siena, O. Zeda 1994: Mid-ocean ridge and supra-subduction affinities in the ophiolitic belts from Albania. – Ofioliti, 19, pp. 77–96.

Beccaluva, L., G. Macciotta, G.B. Piccardo, O. Zeda 1989: Clinopyroxene composition of ophiolite basalts as petrogenetic indicator. – Chemical Geology, 77, pp. 165–182.

Bédard, J.H., K. Lauziere, A. Tremblay, A. Sangster 1998: Evidence for forearc seafloor spreading from the Betts Cove ophiolite, Newfoundland: Oceanic crust of boninitic affinity. – Tectonophysics, 284, pp. 233–245.

Bloomer, S.H., B. Taylor, C.J. MacLeod, R.J. Stern, P. Fryer, J.W. Hawkins, L. Johnson 1995: Early arc volcanism and the ophiolite problem: a perspective from drilling in the Western Pacific. – In: Taylor, B., J. Natland (Eds), Active Margins and Marginal Basins of theWestern Pacific, 88. American Geophysical Union Geophysical Monograph, pp. 1–30.

Çelik, Ö.F., A. Marzoli, R. Marschik, M. Chiaradia, F. Neubauer, I. Öz 2011: Early-Middle Jurassic intra-oceanic subduction in the Izmir–Ankara–Erzincan Ocean, northern Turkey. – Tectonophysics, 509, pp. 120–134.

Çelik, Ö.F., M. Chiaradia, A. Marzoli, Z. Billor, R. Marschik 2013: The Eldivan ophiolite and volcanic rocks in the Izmir–Ankara–Erzincan suture zone, Northern Turnkey: Geochronology, whole-rock geochemical and Nd–Sr–Pb isotope characteristics. – Lithos, 172–173, pp. 31–46.

Cosca, M.A., R.J. Arculus et al. 1998: $^{40}Ar/^{39}Ar$ and K–Ar geochronological age constraints for the inception and early evolution of the Izu–Bonin–Mariana arc system. – The Island Arc, 7, pp. 579–595.

Deer, W.A., R.A. Howie, J. Zussman 1992: An Introduction to the Rock Forming Minerals, Seconded. – Longman Scientific and Technical, 696 pp.

Dick, H.J.B., T. Bullen 1984: Chromian spinel as a petrogenetic indicator in abyssal and Alpine-type peridotites and spatially associated lavas. – Contributions to Mineralogy and Petrology, 86, pp. 54–76.

Dilek, Y., H. Furnes, M. Shallo 2008: Geochemistry of the Jurassic Mirdita Ophiolite (Albania) and the MORB to SSZ evolution of a marginal basin oceanic crust. – Lithos, 100, pp. 174–209.

Dilek, Y., P. Thy 2009: Island arc tholeiite to boninitic melt evolution of the Cretaceous Kizildag (Turkey) ophiolite: Model for multi-stage early arc–forearc magmatism in Tethyan subduction factories. – Lithos, 113, pp. 68–87.

Droop, G.T.R. 1987: A general equation for estimating Fe^{3+} concentrations in ferromagnesian silicates and oxides from microprobe analyses, using stoichiometric criteria. – Mineralogical Magazine, 51, pp. 431–435.

Encarnacion, E. 2004: Multiple ophiolite generation preserved in the northern Philippines and the growth of an island arc complex. – Tectonophysics, 392, pp. 103–130.

Ghazi, A.M., A.A. Hassanipak 2000: Petrology and geochemistry of the Shahr-Babak ophiolite, Central Iran. – Geological society of America, Special paper, 349, pp. 485–497.

Ghazi, A. M., E.A. Pessagno, A.A. Hassanipak, S.M. Kariminia, R.A. Duncan, H.A. Babaie 2003: Biostratigraphic zonation and 40Ar/39Ar ages for the Neo-Tethyan Khoy ophiolite of NW Iran. – Palaeogeography, Palaeoclimatology, Palaeoecology, 193, pp. 311–323.

Godard, M., J.M. Dautria, M. Perrin 2003: Geochemical variability of the Oman ophiolite lavas: Relationship with spatial distribution and paleomagnetic directions. – Geochemistry, Geophysics, Geosystems, 4, 8609, http://dx.doi.org/10.1029/2002GC000452,15 pp.

Göncüoglu, M.C., K. Sayit, U.K. Tekin 2010: Oceanization of the northern Neotethys: Geochemical evidence from ophiolitic mélange basalts within the Izmir–Ankara suture belt, NW Turkey. – Lithos, 116, pp. 175–187.

Hajialioghli, R., M. Moazzen 2014: Supra-subduction and mid-ocean ridge peridotites from the Piranshahr area, NW Iran. – Journal of Geodynamics, doi.org/10.1016/j.jog.2014.06.003

Hassanipak, A., M. Ghazi 2000: Petrology, geochemistry and tectonic setting of the Khoy ophiolite, northwest Iran: Implications for Tethyan tectonics. – Journal of Asian Earth Sciences, 18, pp. 109–121.

Helz, R.T. 1973: Phase reactions of basalts in their melting range at PH_2O=5kb as a function of oxygen fugacity. – Journal of Petrology, 17, pp. 139–193.

Ilkhani, M. 2013: Petrology and geochemistry of peridotites from the Naghadeh area, NW Iran. M.Sc. Thesis. – University of Tabriz, Iran, 138 pp.

Ishii, T., P.T. Robinson, H. Maekawa, R. Fiske 1992: Petrological studies of peridotites from diapiric serpentinite seamounts in the Izu–Ogasawara–Mariana forearc, Leg 125. – In: Fryer, P., J.A. Pearce, L.B. Stokking et al. (Eds): Proceedings of the Ocean Drilling Program Scientific Results, 125, pp. 445–486.

Johnson, K.T.M., H.J.B. Dick 1992: Open system melting and temporal and spatial variation of peridotite and basalt at the Atlantis II Fracture Zone. – Journal of Geophysical Research, 97, pp. 9219–9241.

Johnson, K.T.M., H.J.B. Dick, N. Shimizu 1990: Melting in the oceanic upper mantle: Anion microprobe study of diopsides in abyssal peridotites. – Journal of Geophysical Research, 95, pp. 2661–2678.

Kananian, A., T. Juteau, H. Bellon, A. Darvishzadeh, M. Sabzehi, H. Whitechurch, L.E. Ricou 2001: The ophiolite of Kahnuj (western Makran, southern Iran): new geological and geochronological data. – Comptes Rendus de l'Académie des Sciences – Series IIA – Earth and Planetary Science, 332, pp. 543–552.

Khalatbari-Jafari, M., T. Juteau, H. Bellon, H. Emami 2003: Discovery of two ophiolite complexes of different ages in the Khoy area (NW Iran). – Comptes Rendus Geoscience, 335, pp. 917–929.

Khalatbari-Jafari, M., T. Juteau, H. Bellon, H. Whitechurch, J. Cotton, H. Emami 2004: New geological, geochronological and geochemical investigations on the Khoy ophiolites and related formations, NW Iran. – Journal of Asian Earth Science, 23, pp. 507–535.

Khalatbari-Jafari, M., T. Juteau, J. Cotton 2005: Petrological and geochemical study of the late Cretaceous ophiolite of Khoy (NW Iran), and related geological formations. – Journal of Asian Earth Sciences, 27, pp. 465–502.

Kornprobst, J., D. Ohnenstetter, M. Ohnenstetter 1981: Na and Cr contents in Cpx from peridotites: A possible discriminant between sub-continental and sub-oceanic mantle. – Earth and Planetary Science Letters, 53, pp. 241–254.

Le Bas, N.J. 1962: The role of aluminum in igneous clinopyroxenes with relation to their parentage. – American Journal of Science, 260, pp. 267–288.

Leterrier, J., R.C. Maury, P. Thonon, D. Girard, M. Marchal 1982: Clinopyroxene composition as a method of identification of the magmatic affinities of Paleo-volcanic series. – Earth and Planetary Science Letters, 59, pp. 139–154.

Mehdipour Ghazi, J., M. Moazzen, M. Rahghoshay, H. Shafaii Moghadam 2010: Mineral chemical composition and geodynamic significance of peridotites from Nain ophiolite, central Iran. – Journal of Geodynamics, 49, pp. 261–270.

Moazzen, M., S. Alchalan, R. Hajialioghli, T. Morishita, M. Rezaei 2012: Ophiolitic peridotites from the Western Khoy ophiolitic complex, NW Iran; Petrological and geochemical characteristics and application for connecting the Baft-Khoy and Izmir–Ankara–Erzincan sutures. – In: Proceedings of international earth science colloquium on the Aegean Region, 1–5 October 2012, Izmir, Turkey, p. 9.

Monsef, I., M. Rahgoshay, M. Mohajjel, H. Shafaii Moghadam 2010: Peridotites from the Khoy Ophiolitic Complex, NW Iran: Evidence of mantle dynamics in a supra-subduction-zone context. – Journal of Asian Earth Sciences, 38, pp. 105–120.

Morimoto, N., J. Fabries, A.K. Ferguson, I.V. Ginzburg, M. Ross, F.A. Sefert, J. Zussman, K. Aoki, G. Gottardi 1988: Nomenclature of Pyroxenes. – Mineralogical Magazine, 52, pp. 535–550.

Nisbet, E.G., J.A. Pearce 1977: Clinopyroxene composition in mafic lavas from different tectonic settings. – Contributions to Mineralogy and Petrology, 63, pp. 149–160.

Okay, A.I. 1989: Alpine-Himalayan blueschists. – Annual Reviews Earth and Planetary Sciences, 17, pp. 55–87.

Okay, A.I., O. Tüysüz 1999: Tethyan sutures of northern Turkey. – In: Durand, B., L. Jolivet, E. Horvath, M. Seranne (Eds): The Mediterranean Basins: Tertiary Extension within the Alpine Orogen. Geological Society of London Special Publication, 156, pp. 475–515.

Omrani, H., M. Moazzen, R. Oberhansli, T. Tsujimori, R. Bousquet, M. Moayyed 2013: Metamorphic history of glaucophane-paragonite-zoisite eclogites from the Shanderman area, northern Iran. – Journal of Metamorphic Geology, 31, pp. 791–812.

Pearce, J.A., S.R. Van der Laan, R.J. Arculus, B.J. Murton, T. Ishii, D.W. Peate, I.J. Parkinson 1992: Boninite and harzburgite from Leg 125 (Bonin–Mariana forearc): A case study of magma genesis during the initial stages of subduction. – In: Fryer, P., J.A. Pearce, L.B. Stokking (Eds): Proceedings of the Ocean Drilling Program, Scientific Results. Ocean Drilling Program, College Station, Texas, pp. 623–659.

Schweitzer, E.L., J.J. Papike, A.E. Bence 1974: Statistical analysis of clinopyroxenes from deepsea basalts. – American Mineralogist, 64, pp. 501–513.

Shafaii Moghadam, H., R.J. Stern 2011: Geodynamic evolution of upper Cretaceous Zagros ophiolites: Formation of oceanic lithosphere above a nascent subduction zone. – Geological Magazine, 148, pp. 762–801.

Shafaii Moghadam, H., R.J. Stern, M. Rahgoshay 2010: The Dehshir ophiolite (central Iran): Geochemical constraints on the origin and evolution of the Inner Zagros ophiolite belt. – Geological Society of America, 122, pp. 1516–1547.

Soesoo, A. 1997: A multivariate statistical analysis of clinopyroxene composition: Empirical coordinates for the crystallisation PT-estimations. – Geological Society of Sweden (Geologiska Föreningen), 119, pp. 55–60.

Stöcklin, J. 1977: Structural correlation of the Alpine ranges between Iran and Central Asia. – Mémoires Société Géologique de France, 8, pp. 333–353.

Topuz, G., G. Göçmengil, Y. Rolland, F. Çelik, T. Zack, A.K. Schmitt 2013a: Jurassic accretionary complex and ophiolite from northeast Turkey: No evidence for the Cimmerian continental ribbon. – Geology, 41, pp. 255–258.

Topuz, G., Ö.F. Çelik, A.M.C. Şengör, I.E. Altintaş, T. Zack, Y. Rolland, M. Barth 2013b: Jurassic ophiolite formation and emplacement as backstop to a subduction-accretion complex in northeast Turkey, the Refahiye ophiolite, and relation to the Balkan ophiolites. – American Journal of Science, 313, pp. 1054–1087.

Van der Laan, S.R., R.J. Arculus, J.A. Pearce, B.J. Murton 1992: Petrography, mineral chemistry, and phase relations of the basement boninite series of site 786, Izu–Bonin forearc. – In: Fryer, P., J.A. Pearce, L.B. Stokking et al. (Eds): Proceedings of the Ocean Drilling Program, Scientific Results, 125, College Station, Texas, pp. 171–201.

Whitney, D.L., B.W. Evans 2010: Abbreviations for names of rock-forming minerals. – American Mineralogist, 95, pp. 185–187.

Zanchetta, S., A. Zanchi, I. Villa, S. Poli, G. Muttoni 2009: The Shanderman eclogites: A Late Carboniferous high-pressure event in the NW Talesh Mountains (NW Iran). – Geological Society of London, Special Publications, 312, pp. 57–78.